REPORT DOCUMENTATION PAGE

Form Approved
OMB NO. 0704-0188

1. AGENCY USE ONLY (Leave Blank)	2. REPORT DATE	3. REPORT TYPE AND DATES COVERED
		Reprint

4. TITLE AND SUBTITLE
Internal Pressure and Surface Tension of Bare and Hydrogen Coated Silicon Nanoparticles

5. FUNDING NUMBERS
DAAD19-01-1-0503

6. AUTHOR(S)
See Attached

7. PERFORMING ORGANIZATION NAME(S) AND ADDRESS(ES)
UNIVERSITY OF MINNESOTA – MINNEAPOLIS
450 McNamar Alumni Center
Minneapolis, MN 55455

8. PERFORMING ORGANIZATION REPORT NUMBER

9. SPONSORING / MONITORING AGENCY NAME(S) AND ADDRESS(ES)
U. S. Army Research Office
P.O. Box 12211
Research Triangle Park, NC 27709-2211

10. SPONSORING / MONITORING AGENCY REPORT NUMBER
42323.22-EG-NNI

11. SUPPLEMENTARY NOTES
The views, opinions and/or findings contained in this report are those of the author(s) and should not be construed as an official Department of the Army position, policy or decision, unless so designated by other documentation.

12 a. DISTRIBUTION / AVAILABILITY STATEMENT
Approved for public release; distribution unlimited.

12 b. DISTRIBUTION CODE

13. ABSTRACT (Maximum 200 words)
See Attached

14. SUBJECT TERMS

15. NUMBER OF PAGES

16. PRICE CODE

17. SECURITY CLASSIFICATION OR REPORT	18. SECURITY CLASSIFICATION ON THIS PAGE	19. SECURITY CLASSIFICATION OF ABSTRACT	20. LIMITATION OF ABSTRACT
UNCLASSIFIED	**UNCLASSIFIED**	**UNCLASSIFIED**	**UL**

Internal pressure and surface tension of bare and hydrogen coated silicon nanoparticles

T. Hawa and M. R. Zachariah[a)]
Department of Mechanical Engineering and Department of Chemistry, University of Maryland, College Park, Maryland and National Institute of Standards and Technology, Gaithersburg, Maryland

(Received 12 May 2004; accepted 2 August 2004)

We present a study of internal pressure and surface tension of bare and hydrogen coated silicon nanoparticles of 2–10 nm diameter as a function of temperature, using molecular dynamics simulations employing a reparametrized Kohen–Tully–Stillinger interatomic potential. The internal pressure was found to increase with decreasing particle size but the density was found to be independent of the particle size. We showed that for covalent bond structures, changes in surface curvature and the associated surface forces were not sufficient to significantly change bond lengths and angles. Thus, the surface tension was also found to be independent of the particle size. Surface tension was found to decrease with increasing particle temperature while the internal pressure did not vary with temperature. The presence of hydrogen on the surface of a particle significantly reduces surface tension (e.g., drops from 0.83 J/m^2 to 0.42 J/m^2 at 1500 K). The computed pressure of bare and coated particles was found to follow the classical Laplace–Young equation. © *2004 American Institute of Physics.* [DOI: 10.1063/1.1797073]

I. INTRODUCTION

Nanoclusters of silicon are of considerable interest due to their potential application in optoelectronics. At this length scale, quantum confinement effects play an important role in the electronic properties which has prompted studies in understanding the change in electronic and transport properties of materials and the structures as a function of size.[1–4] Of course, the desirability of these materials places a burden on developing methods for preparing them in the desired size, shape, and purity. Nanoparticles and nanocrystals of Si can be prepared by plasma enhanced chemical vapor deposition.[5–7] Laser ablation of Si wafer[8] and thermal vaporization of melted Si (Ref. 9) may also be used to prepare Si nanoclusters. In many cases these methods result in a silicon oxide layer on the nanoclusters which may be removed by etching with Hydrofluoric (HF).

For production of nanoparticles by gas-phase condensation processes, the high concentrations of fine particles causes rapid coagulation. The ultimate size of the spherical primary particles and the growth of agglomerates are determined by the competition between the time for particle-particle collisions and coalescence.[10] Particles will coalesce before another collision event occurs when the characteristic collision time between particles is smaller than the characteristic coalescence time. On the other hand, chain aggregates will be formed when the collision time is less than the characteristic coalescence time.

$$\tau_{\text{coalescence}} < \tau_{\text{collision}} \rightarrow \text{Spherical particle},$$

$$\tau_{\text{coalescence}} > \tau_{\text{collision}} \rightarrow \text{Agglomerate}.$$

In principle then, by either controlling the characteristic coalescence time or the collision time it is possible to control the particle morphology and particle size. The two most obvious ways to control the primary particle size is to either change the characteristic collision time by dilution or change the coalescence time by changing particle temperature.

Another strategy, however, would be to make particle-particle collisions nonreactive. In a recent molecular dynamics study Hawa and Zachariah[11] showed that the presence of a hydrogen passivation surface on silicon nanoparticles (size 200–6400 Si atoms at 300–1800 K) resulted in particle bounce during collision even when the particles were liquid droplets. That work also showed that there was a critical approach energy for reaction which increases with increasing particle size but decreases with increasing particles temperature.

The rate at which two colliding particles coalesce has been modeled by both phenomenological[12–17] and molecular dynamics methods[18] which has resulted in simple to apply kinetic laws. For example, the characteristic coalescence time calculated from a solid state diffusion model is written as[12,13,15]

$$\tau_f = \frac{3kT_pN}{64\pi\sigma D}, \tag{1}$$

where T_p is the particle temperature, N is the number concentration, D is the solid-state diffusion coefficient reported as an Arrhenius function of the temperature,[16] and σ is the surface tension of the particle. For viscous flow, the coalescence time is given by[17]

$$\tau_f = \frac{\eta d_p}{\sigma}, \tag{2}$$

a)Author to whom correspondence should be addressed. Electronic mail: mrz@umd.edu

where d_p is the diameter of the particle and η is the temperature dependent viscosity.

In looking at the above two kinetic laws it is apparent that surface properties play an important role. The driving force for coalescence is in fact the minimization of the surface free energy and it is not surprising then that surface tension appears as a parameter in both equations, and the diffusion constant is obviously important in the solid-state coalescence event.

Given that the driving force for coalescence is the minimization of the surface free energy, it is important to understand the effect of hydrogen surface passivation on the surface tension and the diffusion coefficient of the particles as well as the role of particle size. Although hydrogenated amorphous silicon has found a variety of technological applications, and has been studied extensively,[19] these previous studies focused on the electronic and optical properties,[20–26] thin film growth,[27,28] and the deposition of clusters on hydrogenated surface.[29–38] To our best knowledge, surface tension and diffusion coefficient of hydrogenated Si nanoparticles have not been reported on.

In this paper we investigate the role of hydrogen passivation on physical properties, such as surface tension, internal pressure, and surface diffusion. We use classical molecular dynamics simulation using the reparametrized Kohen–Tully–Stillinger (KTS) potential for the silicon-hydrogen system.[11,39]

II. COMPUTATIONAL MODEL AND SIMULATION PROCEDURE

Recent geometric optimizations and molecular dynamics (MD) simulations based on an empirical tight-binding approach for fully and partially hydrogenated Si nanocrystals showed that the structural properties were not very size dependent, unlike electronic properties.[40,41] However, hydrogenation has been shown to stabilize the structure of Si_n clusters ($n=2$ to 10) through termination of dangling bonds.[42] Prior studies using molecular dynamics have been used to study surface energies of nanoclusters. For example, studies of solid and liquid silica particles show that the surface tension was independent of particle size over a wide range of temperature.[43] On the other hand, MD studies of Lennard-Jones (LJ) clusters[44] and a variable charge transfer MD for aluminum[45] showed that surface tension decreased with decreasing particle size.

This study involves atomistic simulations using classical molecular dynamics. For this study we use the reparametrized KTS interatomic potential for the silicon-hydrogen system developed by Hawa and Zachariah.[11] This interatomic potential for silicon was originally developed by Stillinger and Weber[46] and extended by Kohen *et al.*[39] to include Si-H and H-H interactions. Similar sets of potential energy functions have also been developed by Murty and Atwater,[47] Ohira and co-workers[33,34,36] and Ramalingam *et al.*[37] where a Tersoff-type potential[48–51] was extended to describe interatomic interactions in the Si:H system. This extended version of the Tersoff potential has been tested successfully for its accuracy in describing the Si:H system in several earlier studies; however, the simulation of liquid silicon has not been well described by the potential.[48] By contrast, the reparametrized KTS potential, which is the extended spherical wave Stillinger and Weber (SW) potential, was designed to describe interactions in both solid and liquid forms of silicon. Since most synthesis processes leading to cluster formation occur at high temperature, cluster growth by coalescence is dominated by liquidlike characteristics, and the accuracy of the SW potential increases with increasing particle size or temperature, we use this potential form for our investigations. The reparametrized KTS potential energy is a sum of two and a three-body interactions, and the details of the model and its parameters are given in the literature (Hawa and Zachariah).[11]

All simulations were run on an Origin computer running up to 16 processors. The trajectories of all the atoms are determined by integrating the equation of motion according to the velocity form of the Verlet algorithm[52] with rescaling of atomic velocities at each time step to achieve temperature control. Time steps of 0.5 and 0.05 fs were typically used for both pure silicon, and for hydrogen coated particles to ensure energy conservation, and the Verlet neighbor list with parallel architecture was employed in all the simulations. The neighbor list was renewed every ten steps. The simulations take place in a spherical cavity of 10 nm radius with an elastic boundary condition.

The first step in the equilibration process was to prepare pure silicon particles of various sizes (2, 3, 4, 6, and 10 nm diameters) (200, 800, 1600, 6400, 25 600 Si atoms) at 300 K. After the angular momentum was removed, the particle temperature was raised to 2100 K using constant temperature MD for 50 ps. The particle temperature was then reduced slowly to 300 K and equilibrated for 50 ps. The next step was to coat the particles with hydrogen atoms. Since the particles were already equilibrated, almost all surface atoms had a coordination number of three. A hydrogen atom was placed on each surface silicon atoms at a distance of 1.5 Å to prepare fully hydrogen coated particles, while the particle temperature was maintained at 300 K for 10 ps. Any hydrogen atoms that were released from the surface were removed from the simulation, and the dynamics repeated for 10 ps. As a result, the numbers of hydrogens placed on the silicon particles composed of 200, 800, 1600, and 6400 Si atoms was 74, 211, 367, and 785, respectively. For the preparation of partially hydrogen coated particles, appropriate number of hydrogen atoms were randomly removed from the particles, and the dynamics repeated for 10 ps for equilibration. After generating the hydrogen monolayer on the silicon particles, the temperature of the particles was slowly raised to the desired temperatures of 1000, 1500, or 1800 K and maintained at constant temperature for 50 ps. For the last step in the preparation process, the simulations were switched to a constant energy calculation for 20 ps. If the average temperature of the particle deviated by more than 10 K over this period, the equilibration process was repeated until the particle temperature deviated by less than 10 K. An external and cross-sectional view of an equilibrated nanoparticle, consisting of 6400 Si atoms, coated with 785 H atoms, corresponding to roughly a 6 nm particle are shown in Fig. 1. The properties such as radial pressure, density, surface tension, and diffusiv-

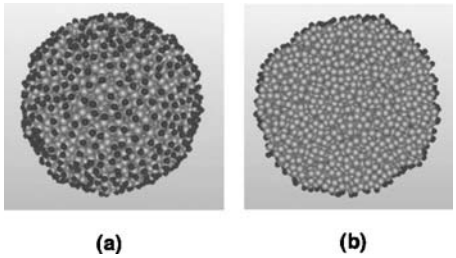

FIG. 1. A 6 nm hydrogen-coated silicon nanoparticles (6400 Si+785 H atoms): (a) external view, (b) cross-sectional view.

ity were computed, and the pressure and density were averaged by collecting 200 snapshots over 40 ps.

III. RESULTS AND DISCUSSION

A. Density

The radial density distributions for fully and 50% hydrogen coated and bare 4 nm silicon particles at 1500 K, is shown in Fig. 2. The hydrogen density profiles of both 100% and 50% coated particles show that the maximum values of the hydrogen density is achieved at the surface of the silicon particle and that no hydrogen exists inside of either particle. The peak value in hydrogen densities occurs at the same radial location independent on hydrogen coverage. Naturally the magnitude in density of the 50% coating is lower than that of a fully coated particle and the ratio of the areas under the distribution curves of the fully coated particle to that of a 50% coated particle is two. The fact that the higher coverage condition seemed to have a density profile that was wider, and biased toward the interior of the particle, might indicate that the silicon atoms that have hydrogen attached are more likely to sit out of the surface, while the unpassivated atoms recede toward the interior. On the other hand, the silicon density profiles for all bare, fully, and partially coated particles are indistinguishable except near the surface. Prior work using an empirical tight-binding approach for studying the structure of fully and partially hydrogenated Si nanocrystals (Si$<$706 atoms) found that there was only a very small lattice strain, of the order 10^{-4} to 10^{-3},[41] in agreement with x-ray diffraction measurements,[40] and confirms that the density profiles should be independent of surface coverage. Figure 3 shows the density profiles of 3 and 6 nm bare silicon particles at 1800 K. It can be seen that the average densities do not depend on the size of the particles. The average density of the particle at 1800 K is about 2.57 g/cc, and the value is consistent with the density recently measured for bulk pure molten silicon (2.55 g/cc).[53] Our studies show neither particle size or hydrogen surface coverage have an effect on silicon particle density.

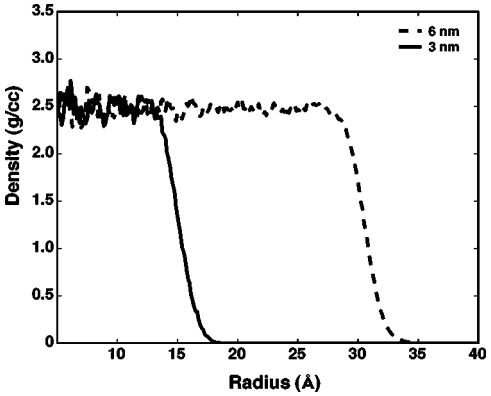

FIG. 3. Radial density profile for a 3 and 6 nm hydrogen coated silicon particle at 1800 K.

B. Diffusion

Self-diffusion coefficient D is calculated from the slope of the atomic mean-square displacement (MSD):

$$\mathrm{MSD}=\frac{1}{N}\sum_{i=1}^{N}[r_i(t)-r_i(0)]^2, \tag{3}$$

$$D=\frac{1}{6}\frac{d}{dt}(\mathrm{MSD}), \tag{4}$$

where N is the number of atoms in the particle and r is the position of each atom. Since the curvature in the MSD toward an asymptote results from the finite nature of the cluster, the self-diffusion coefficient can be evaluated from the initial slope of the MSD in Eq. (3). Figure 4 shows the self-diffusion coefficients of both bare and fully hydrogenated 6 nm particles at 1000, 1500, and 1800 K. We find that the presence of hydrogen on the surface of a silicon particle slightly increases the diffusivity of silicon atoms of a coated

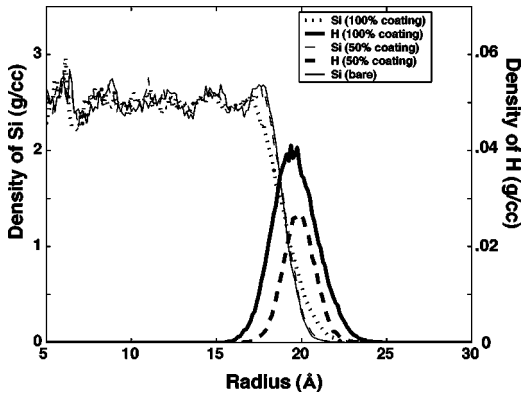

FIG. 2. Radial density profiles of fully and 50% hydrogen coated and bare 4 nm silicon particle at 1500 K.

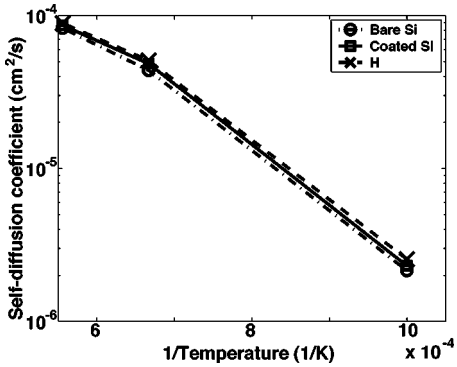

FIG. 4. Self-diffusion coefficients of both bare and coated 6 nm particles at 1000, 1500, and 1800 K.

particle by about 5–15% over the temperature range sampled. Since our reparametrized KTS potential is an extension of SW potential, our results show agreement with the earlier work by Zachariah *et al.*[54] who used the SW potential for Si clusters up to 480 atoms. By comparing the simulation results with the experimental data of surface self-diffusion,[55–57] they found substantial discrepancy in the bulk experimental data. The SW potential is known to underpredict the binding energy in bulk silicon that would tend to increase the computed surface diffusion coefficient. However, their results showed agreement with those of tight-binding molecular dynamics.[58]

The self-diffusion coefficient of hydrogen atoms is also shown in Fig. 4. We find that hydrogen diffusivity is essentially the same as that of silicon diffusivity. Variable temperature scanning tunnel microscope (STM) measurements on low hydrogen coverage silicon films at temperatures ranging from 300 to 700 K showed that individual hydrogen atoms became mobile at around 570 K, and that rate of hopping along the dimer rows was consistent with an activation energy of 1.68 ± 0.15 eV.[59] In a related study, an upper bound of $D(T=740\ \mathrm{K}) < 10^{-9}\ \mathrm{cm}^2/\mathrm{s}$ was obtained.[60] Reider *et al.* employed an altogether different experimental approach and found effectively the same barrier height ($E_a = 1.5 \pm 0.2$ eV) and a preexponential factor D_0 of $10^{-3}\ \mathrm{cm}^2/\mathrm{s}$ using the method of second-harmonic diffraction from adsorbate gratings.[61] Using these experimental values we estimate a diffusion coefficient (hopping) for H at 1000 K of $\sim 2 \times 10^{-11}\ \mathrm{cm}^2/\mathrm{s}$, which is much lower than our simulation results of the self-diffusion coefficient of hydrogen atoms in Fig. 4. This implies that the surface hydrogen mobility directly reflects the mobility of its silicon anchor, and H hopping rate is negligible at our temperature range, relative to Si self-diffusion.

C. Pressure

The internal pressures are computed using the Irving-Kirkwood pressure tensor extended to a spherical symmetric system as shown by Thompson.[44] The normal component to the spherical surface of the pressure $P_N(r)$ is given by

$$P_N(r) = P_K(r) + P_U(r), \tag{5}$$

where $P_K(r)$ and $P_U(r)$ are kinetic and configurational terms, respectively, and are given by

$$\begin{aligned} P_K(r) &= k_B T \rho(r), \\ P_U(r) &= S^{-1} \sum_k f_k, \end{aligned} \tag{6}$$

where k_B is Boltzmann constant, T is a particle temperature, S is the area of spherical surface of radius r, and f_k is the normal component of the force between an atomic pair acting across the surface S. We introduce 800 subspherical calculation surfaces in the spherical computational cavity of 10 nm radius, to compute the configurational term of pressure for every subsphere surface. The accuracy of this method of pressure computation depends on the number of atoms within the subsphere, and therefore quickly diminishes with decreasing radius.

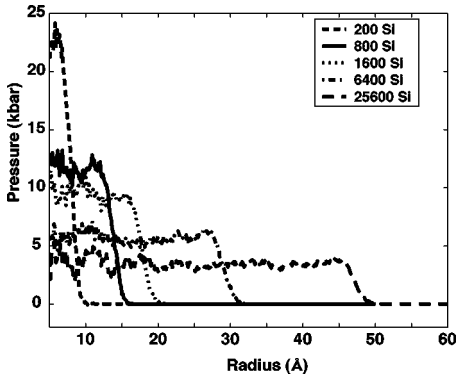

FIG. 5. Radial pressure profile for 2–10 nm silicon particles at 1500 K.

The radial internal pressure distributions for 2 to 10 nm particles at 1500 K are shown in Fig. 5. We see that the internal pressure distributions are very sensitive to the size of the particle at a fixed temperature. The internal pressure increases with decreasing particle size, consistent with the internal pressure profile reported for silica.[43] The effect of temperature are reported in Fig. 6, and show that internal pressure is independent of the particle temperature, even though the kinetic contribution to the normal pressure P_N depends linearly on the temperature. This result is also consistent with the study for silica reported in the literature.[43] The details of these results and its relationship to the well known Laplace–Young equation will be differed, so as to present results on surface tension as these effects are related. The radial pressure distribution at 1000 K shows oscillations near the core of the particle. This is a manifestation of the fact that the number of atoms within the subsphere calculation surface decreases as the inverse cube of the radial distance inward, thus providing poor statistics, and the fact that since the particles are solidlike the atoms have poor mobility. If we could integrate for long enough, one should expect to see the oscillations disappear as they have for liquidlike particles.

Figure 7 shows the pressure profiles of bare, 50%, and fully coated 6 nm particles at 1500 K. The presence of hydrogen on the surface reduces the internal pressure of the coated particle by about 40%. In the definition of the Irving–Kirkwood pressure tensor, the attractive forces make a

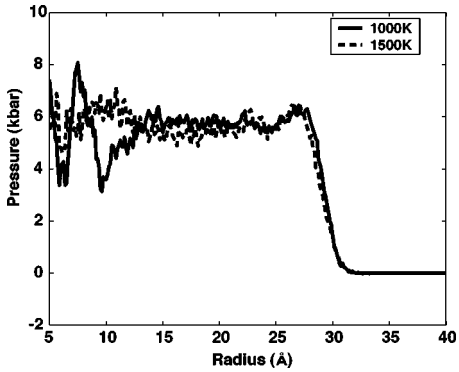

FIG. 6. Radial pressure profile for 6 nm silicon particles at 1000 and 1500 K.

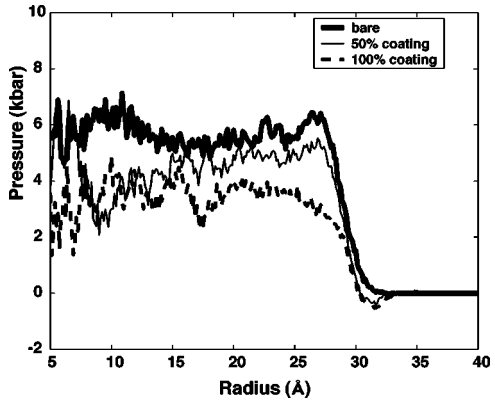

FIG. 7. Radial pressure profile for 6 nm bare and 50% and fully coated silicon particles at 1500 K.

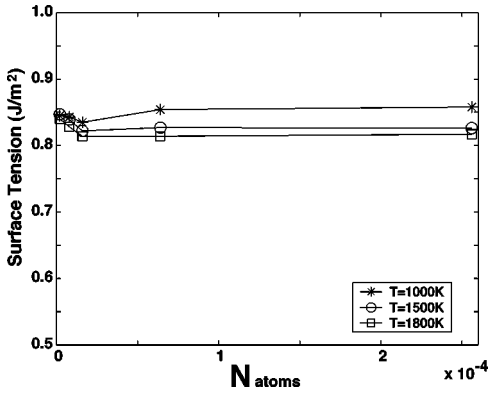

FIG. 9. Surface tension of bare silicon particles as a function of particle size at 1000, 1500, and 1800 K.

negative contribution to the pressure, while repulsive forces make a positive contribution. Thus a decrease in pressure indicates that the bond lengths of all atoms in the particle are on average elongated by the presence of hydrogen on the surface of the particles.

Figure 8 shows that the average bond length for surface atoms for both bare and coated silicon as a function of particle size at 1500 K. We can clearly see that the average bond lengths of hydrogen coated particles are longer than those of bare particles for all sizes. Moreover, both average surface bond length initially increases with increasing particle size, but that the size dependence disappears by about 4 nm ($\sim$2000 atoms). It is known that the average bond length tends to become shorter with decrease of the coordination number.[62] The similar tendency in the average coordination number has been also pointed out in our previous studies (Zachariah *et al.*[54]).

The average bond lengths of inner 1800 silicon atoms of bare and fully coated particles at 1500 K are 2.4928 and 2.4944 Å, and the ratio of the difference to the bond length of bare particles is 6.4×10^{-4}, in agreement with the strain of 10^{-4} to 10^{-3} obtained from tight-binding calculation of silicon crystals[41] and x-ray diffraction measurements.[40]

D. Surface tension

The surface tension σ is computed using the mechanical approach reported by Thompson *et al.*[44]

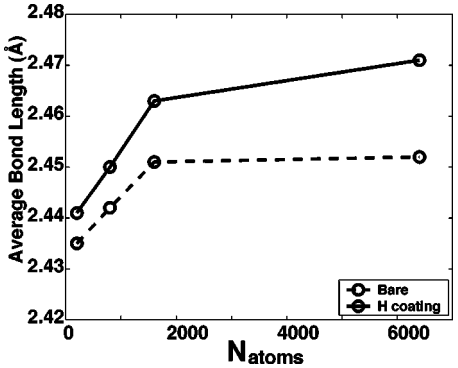

FIG. 8. Average bond length of bare and hydrogen coated surface silicon atoms as a function of particle size at 1500 K.

$$\sigma=\left[-\frac{(p_L-p_G)^2}{8}\int_0^\infty r^3\frac{dP_N(r)}{dr}dr\right]^{1/3}, \tag{7}$$

where p_G is gas pressure outside the particle and p_L is pressure inside the particle. Since almost all contribution to the surface tension comes from the surface pressure, we estimated the p_L as the average pressure near the surface of the particle and p_G can be ignored.

The surface tension as a function of particle size is shown in Fig. 9. It is interesting to note that the surface tension does not depend on particle size, and is qualitatively consistent with the study for silica.[43] Since the surface tension depends on both the calculated pressure and density profiles, the accuracy of the surface tension diminishes with decreasing particle size.

Thompson *et al.*[44] and Sonwane *et al.*[45] in their work reported that surface tension for Lennard-Jones clusters and aluminum, respectively, decreased with decreasing particle size. We believe the distinction between LJ and aluminum versus silicon and silica can be attributed to the nature of bonding. Silica and silicon are covalent structures, whose bonding is highly directional. Changes in surface curvature and the associated surface forces are not sufficient to significantly change bond lengths and angles. This implies that the nature of covalent bonded surfaces is to first order size invariant. In contrast LJ and possibly metals are more able to find different bonding configurations as the surface curvature changes, thus resulting in changes to surface energy as a function of particle size.

In order to evaluate this argument, we ignore the third-body effect in the reparametrized KTS potential so that the potential behaves like an LJ cluster. Figures 10 and 11 show the radial internal pressure distribution for various particle sizes, and the surface tension as a function of the particle size at fixed temperature. Both the pressure and surface tension values are normalized by the maximum values obtained in the simulation. The internal pressures obtained are qualitatively similar to that obtained with the full potential (see Fig. 5). However, the surface tension shows a size dependence that is similar to that observed by Thompson *et al.* for LJ clusters and Sonwane *et al.* for aluminum. This implies that indeed, consistent with our conjecture, directionally bonded

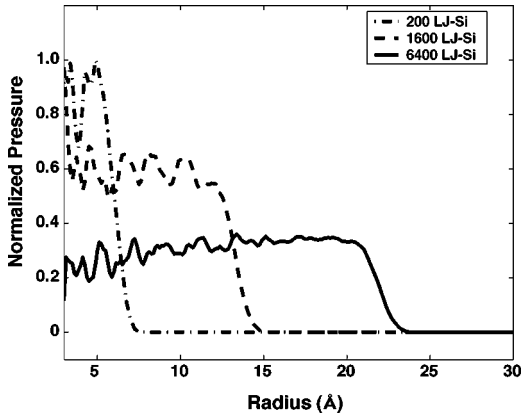

FIG. 10. Radial pressure profile neglecting the third body term for various sizes for at 1500 K.

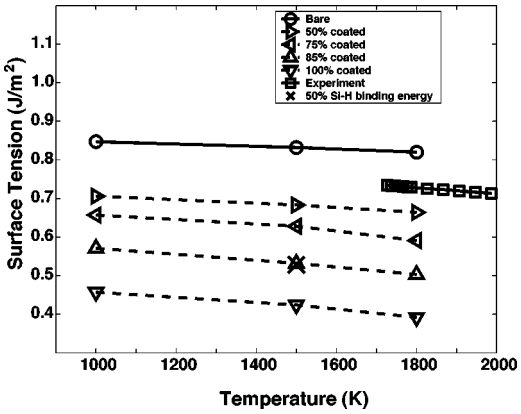

FIG. 12. Surface tension of bare and partially and fully coated silicon particles with experimental results and the case of a half Si–H bonding energy.

materials should not show any size dependent surface tension effects.

From Fig. 9 we also see that the surface tension decreases with increasing particle temperature for the pure silicon particles. This trend is also observed for hydrogenated particles shown in Fig. 12. Since we have shown that surface tension is size invariant, results presented in Fig. 12 are the averages of results for 2 to 10 nm particles. The surface tension is the energy required to incrementally increase the surface area. Since it is easier to increase surface area at higher temperatures when the atoms are more mobile, the surface tension must decrease with increasing temperature. Experimental results[63] of surface tension of bulk silicon as a function of temperature are also plotted in Fig. 12 and show the same temperature dependence and are of similar magnitude (~15%).

Figures 9 and 12 also show the role of hydrogen atoms on surface tension. With increasing hydrogen coverage the surface tension decreases. Conceptually the surface tension is a bulk measure of the energy of a surface atom relative to interior atoms. At the atomic scale the attractive forces between atoms interior to a particle are shared with all neighboring atoms. However, those on the surface have fewer neighboring atoms above the surface, and exhibit stronger attractive forces upon their nearest surface and subsurface neighbors. Since this enhancement of the interatomic attractive forces at the surface is called as surface tension, the presence of hydrogen atoms on the silicon surface produces attractive forces above the silicon surface and reduces the surface tension of the silicon particle.

Since the surface tension is a measure of the energy of surface atoms, which can be changed by the nature of the surface termination bond, one can in principle tune surface tension through attachment of an appropriate ligand. For example, if we arbitrarily change the bond energy of Si–H to half its nominal value, we get the result shown by the symbol (X) in Fig. 12, which is an increase in surface tension of about 30%. Since the surface tension is a key parameter in the kinetics of nanoparticle coalescence as described by Eqs. (1) and (2), the use of surface manipulation may afford a new opportunity which to this point has been unexplored to affect growth rates of gas phase generated nanoparticles.

Finally we turn our attention to the well known Laplace–Young equation, which is widely used for droplets to describe the relationship between pressure, surface tension, and size:

$$p_L - p_0 = 2\sigma/r. \tag{8}$$

Figure 13 shows the pressure change as a function of radius using Eq. (8) at 1500 K and compares it with the internal pressure obtained from Fig. 7. We can see that the internal pressure computed from Laplace–Young equation is in excel-

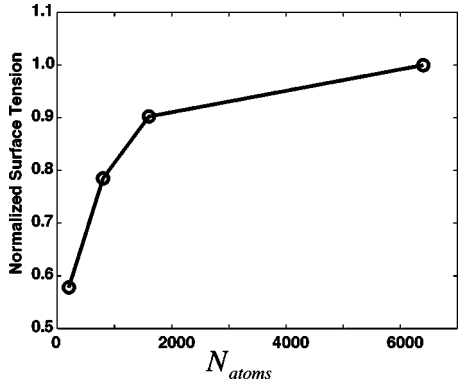

FIG. 11. Surface tension neglecting the third body term for various sized particles at 1500 K.

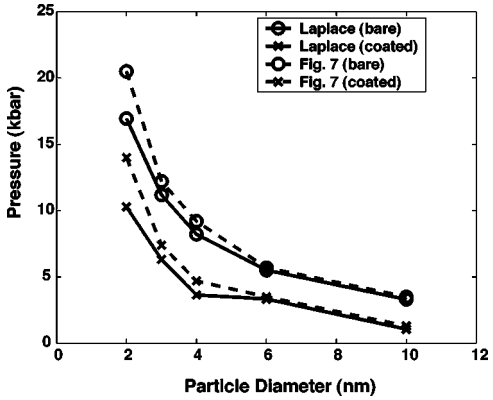

FIG. 13. Comparison of pressure obtained from Laplace–Young equation with Irving–Kirkwood pressure tensor.

lent agreement with our MD results for both the coated and uncoated cases, with the exception of very small particle sizes. The results from Fig. 13 also imply the Laplace–Young equation is valid for surface coated particles, i.e., nonhomogeneous particles. Extrapolation of Eq. (8) to very small clusters imply increasing internal pressure to the point of a pressure singularity. In fact, the concept of a surface tension would itself come into question for very small particle sizes. For the purposes of this study we conclude that, over the range of 2–10 nm, the phenomenological description provided by the Laplace–Young equation is valid.

IV. CONCLUSION

Classical molecular dynamics using the reparametrized three-body KTS potential was used to study the internal pressure and surface tension of bare and hydrogen coated silicon nanoparticles. Simulations were performed over a wide range of particle diameters between 2–10 nm and at a temperature of 1000, 1500, and 1800 K. It was found that internal pressure increases with decreasing particle size but is independent of particle temperature. Surface tension decreases with increasing particle temperature but is independent of the particle size. We believe that this result should be generic to covalent bonded structures, whose bond lengths and angles are not easily changed, by changes in surface curvature and associated surface forces. It was observed that the presence of hydrogen on the silicon particle has little effect on surface diffusion, but significantly decreases both internal pressure as well as surface tension. The internal pressure of both bare and coated particles was found to agree with Laplace–Young equation.

ACKNOWLEDGMENTS

This work is supported by NSF Grant No. CTS-0083062, the Army High Performance Computing Research Center DAAD19-01-2-0014, the Minnesota Super-Computer Center, and National Institute of Standards and Technology.

[1] A. P. Alivisatos, Science **271**, 933 (1996).
[2] V. L. Colvin, A. P. Alivisatos, and J. G. Tobin, Phys. Rev. Lett. **66**, 2786 (1991).
[3] A. N. Goldstein, C. M. Echer, and A. P. Alivisatos, Science **256**, 1425 (1992).
[4] J. Shi, S. Gider, K. Babcock *et al.*, Science **271**, 937 (1996).
[5] M. Ehbrecht, B. Kohn, F. Huisken *et al.*, Phys. Rev. B **56**, 6958 (1997).
[6] G. Ledoux, O. Guillois, D. Porterat *et al.*, Phys. Rev. B **62**, 15942 (2000).
[7] G. A. Rechtsteiner, O. Hampe, and M. F. Jarrold, J. Phys. Chem. B **105**, 4188 (2001).
[8] P. Melinon, P. Keghelian, B. Prevel *et al.*, J. Chem. Phys. **107**, 10278 (1997).
[9] L. N. Dinh, L. L. Chase, M. Balooch *et al.*, Phys. Rev. B **54**, 5029 (1996).
[10] W. Koch and S. K. Friedlander, J. Colloid Interface Sci. **140**, 419 (1990).
[11] T. Hawa and M. R. Zachariah, Phys. Rev. B **69**, 035417 (2004).
[12] S. H. Ehrman, S. K. Friedlander, and M. R. Zachariah, J. Aerosol Sci. **29**, 687 (1998).
[13] R. S. Windeler, K. E. J. Lehtinen, and S. K. Friedlander, Aerosol Sci. Technol. **27**, 174 (1997).
[14] R. S. Windeler, K. E. J. Lehtinen, and S. K. Friedlander, Aerosol Sci. Technol. **27**, 191 (1997).
[15] P. Biswas, G. Yang, and M. R. Zachariah, Combust. Sci. Technol. **134**, 183 (1998).
[16] S. K. Friedlander and M. K. Wu, Phys. Rev. B **49**, 3622 (1994).
[17] J. Frenkel, Am. J. Phys. **9**, 385 (1945).
[18] M. R. Zachariah and M. J. Carrier, J. Aerosol Sci. **30**, 1139 (1999).
[19] R. A. Street, *Hydrogenated Amorphous Silicon* (Cambridge University Press, Cambridge, 1991).
[20] S. Zafar and E. A. Schiff, Phys. Rev. Lett. **66**, 1493 (1991).
[21] S. Y. Ren and J. D. Dow, Phys. Rev. B **45**, 6492 (1992).
[22] M. Hirao and T. Uda, Surf. Sci. **306**, 87 (1994).
[23] B. Delley and E. F. Steigmeier, Phys. Rev. B **47**, 1397 (1993).
[24] B. Delley and E. F. Steigmeier, Appl. Phys. Lett. **67**, 2370 (1995).
[25] C. Delerue, G. Allan, and M. Lannoo, Phys. Rev. B **48**, 11024 (1993).
[26] R. Q. Zhang, J. Costa, and E. Bertran, Phys. Rev. B **53**, 7847 (1996).
[27] K. K. Gleason, K. S. Wang, M. K. Chen *et al.*, J. Appl. Phys. **61**, 2866 (1987).
[28] M. J. McCaughey and M. J. Kushner, J. Appl. Phys. **65**, 186 (1989).
[29] P. Kratzer, J. Chem. Phys. **106**, 6752 (1997).
[30] P. Kratzer, B. Hammer, and J. K. Norskov, Phys. Rev. B **51**, 13432 (1995).
[31] P. Kratzer, E. Pehlke, M. Scheffler *et al.*, Phys. Rev. Lett. **81**, 5596 (1998).
[32] F. R. Jeffery, H. R. Shanks, and G. C. Danielson, J. Appl. Phys. **50**, 7034 (1979).
[33] T. Ohira, T. Inamuro, and T. Adachi, Materials Research Society Symposium Proceedings **336**, 177 (1994).
[34] T. Ohira, O. Ukai, T. Adachi *et al.*, Phys. Rev. B **52**, 8283 (1995).
[35] T. Ohira, O. Ukai, M. Noda *et al.*, Materials Research Society Symposium Proceedings **408**, 445 (1996).
[36] T. Ohira, O. Ukai, and M. Noda, Surf. Sci. **458**, 216 (2000).
[37] S. Ramalingam, D. Maroudas, and E. S. Aydil, J. Appl. Phys. **84**, 3895 (1998).
[38] S. Ramalingam, E. S. Aydil, and D. Maroudas, J. Vac. Sci. Technol. B **19**, 634 (2001).
[39] D. Kohen, J. C. Tully, and F. H. Stillinger, Surf. Sci. **397**, 225 (1998).
[40] D. Bellet, G. Dolino, M. Ligeon *et al.*, J. Appl. Phys. **71**, 145 (1992).
[41] D. K. Yu, R. Q. Zhang, and S. T. Lee, J. Appl. Phys. **92**, 7453 (2002).
[42] M. O. Watanabe, H. Murakami, T. Miyazaki *et al.*, Appl. Phys. Lett. **71**, 1207 (1997).
[43] I. V. Schweigert, K. E. Lehtinen, M. J. Carrier *et al.*, Phys. Rev. B **65**, 235410 (2002).
[44] S. M. Thompson, K. E. Gubbins, J. P. R. B. Walton *et al.*, J. Chem. Phys. **81**, 530 (1984).
[45] C. G. Sonwane, J. Mintmire, and M. R. Zachariah, Phys. Rev. B (submitted).
[46] F. H. Stillinger and T. S. Weber, Phys. Rev. B **31**, 5262 (1985).
[47] M. V. R. Murty and H. A. Atwater, Phys. Rev. B **51**, 4889 (1995).
[48] J. Tersoff, Phys. Rev. B **38**, 9902 (1988).
[49] J. Tersoff, Phys. Rev. B **37**, 6991 (1986).
[50] J. Tersoff, Phys. Rev. Lett. **56**, 632 (1988).
[51] J. Tersoff, Phys. Rev. B **39**, 5566 (1989).
[52] L. Verlet, Phys. Rev. B **159**, 98 (1967).
[53] H. Sasaki, E. Tokizaki, K. Terashima *et al.*, Jpn. J. Appl. Phys., Part 1 **33**, 6078 (1994).
[54] M. R. Zachariah, M. J. Carrier, and E. Blaisten-Barojas, J. Phys. Chem. **100**, 14856 (1996).
[55] D. M. Makowiecki and J. B. Holt, Mater. Sci. Res. **13**, 279 (1979).
[56] Y. W. Mo, J. Kleiner, M. B. Webb *et al.*, Surf. Sci. **268**, 275 (1992).
[57] W. M. Robertson, J. Am. Ceram. Soc. **64**, 9 (1981).
[58] C. Z. Wang, Phys. Rev. B **45**, 12227 (1992).
[59] J. H. G. Owen, D. R. Bowler, C. M. Goringe *et al.*, Phys. Rev. B **54**, 14153 (1996).
[60] B. G. Koehler, C. H. Mak, D. A. Arthur *et al.*, J. Chem. Phys. **89**, 1709 (1988).
[61] G. A. Reider, U. Hofer, and T. F. Heinz, Phys. Rev. Lett. **66**, 1994 (1991).
[62] M. Ishimaru, K. Yoshida, and T. Motooka, Phys. Rev. B **53**, 7176 (1996).
[63] H. Sasaki, Y. Anzai, X. Huang *et al.*, Jpn. J. Appl. Phys., Part 1 **34**, 414 (1994).